31st Annual International Conference of the IEEE EMBS
Minneapolis, Minnesota, USA, September 2-6, 2009

Cell Segmentation in Time-Lapse Fluorescence Microscopy with Temporally Varying Sub-cellular Fusion Protein Patterns

Filiz Bunyak[1], Kannappan Palaniappan[1], Vadim Chagin[2,3], M. Cristina Cardoso[2]
[1] Department of Computer Science, University of Missouri-Columbia, Columbia MO 65211-2060, USA
[2] Department of Biology, Technische Universitat Darmstadt, Schnittspahnstr. 10, 64287 Darmstadt, Germany
[3] Institute of Cytology, Russian Academy of Sciences, Tikhoretsky Ave. 4, 194064 St. Petersburg

***Abstract*— Fluorescently tagged proteins such as GFP-PCNA produce rich dynamically varying textural patterns of foci distributed in the nucleus. This enables the behavioral study of sub-cellular structures during different phases of the cell cycle. The varying punctuate patterns of fluorescence, drastic changes in SNR, shape and position during mitosis and abundance of touching cells, however, require more sophisticated algorithms for reliable automatic cell segmentation and lineage analysis. Since the cell nuclei are non-uniform in appearance, a distribution-based modeling of foreground classes is essential. The recently proposed graph partitioning active contours (GPAC) algorithm supports region descriptors and flexible distance metrics. We extend GPAC for fluorescence-based cell segmentation using regional density functions and dramatically improve its efficiency for segmentation from $O(N^4)$ to $O(N^2)$, for an image with N^2 pixels, making it practical and scalable for high throughput microscopy imaging studies.**

I. Introduction

Quantitative analysis of the spatial distribution and temporal dynamics of proteins within living cells is an important step in understanding the interaction between sub-cellular processes and cell behavior. The analysis of cell cycle dependent changes in living cells is only now becoming feasible with the discovery of suitable markers that allow identification of the various cell cycle stages in proliferating cells [6]. Current experimental techniques use fusion proteins in combination with fluorescence time-lapse microscopy imaging to simultaneously label the nucleus for cell detection and mark sub-cellular structures in the nucleus to identify the cell cycle phases. However, depending on the type of labeling used there is wide variability in the textural appearance of the fluorescence markers in the nucleus and possibly throughout the cell, presenting a new set of challenges not anticipated by previously developed approaches for cell segmentation and tracking.

The focus of this paper is on fluorescent labeling using GFP-PCNA which enables cell cycle stages to be distinguished by the associated characteristic sub-nuclear localization of PCNA at different points of the cell cycle in living cells: M-phase or mitosis, followed by G1-phase, early, mid and late S-phase, and G2-phase. GFP-PCNA also produces the most complex distribution of foci patterns across the cell cycle particularly during different stages of the S-phase, but is fairly homogenous during G1- and G2-phases, and very diluted during M-phase.

In order to identify cell cycle phases, individual nuclei need to be detected, segmented and tracked accurately through multiple cycles of cell division. While the varying and complex staining patterns through the cell life cycle increases GFP-PCNA's cell cycle phase discrimination power, also results in increased complexity for cell detection compared to other fluorescently tagged histons like H2B-GFP.

In this paper we describe a novel technique for fluorescent nuclei segmentation using a novel fast implementation of multi-phase graph partitioning active contours. An appearance-based multiple hypothesis tracking algorithm is used to identify the lineage of proliferating cells. The overall proposed system flow is shown in Figure 1. In this paper we do not try to accurately identify the specific stages of the cell cycle but focus on accurately segmenting and tracking the same cell as it undergoes significant appearance and shape changes. The computational challenges include spatiotemporally varying fluorescence labeling patterns, dramatic decrease in (intensity) SNR during mitosis, fluctuation in SNR across the cell cycle and spatially across the cells within a frame, significant deformations in shape particularly during mitosis with the daughter cells having large spatial separation from the mother nucleus, and separation of touching cells.

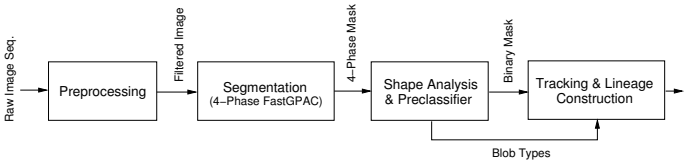

Fig. 1: Process flow chart for fluorescence-based cell segmentation and lineage construction.

II. Segmentation Using Level set-based Fast Graph Partitioning Active Contours (FastGPAC)

There has been extensive recent work on developing a variety of algorithms for automatic cell segmentation and tracking using transmitted light and fluorescent time-lapse microscopy imaging [3], [5], [7]–[10], [15]. Reliable segmentation of nuclei is an important requirement for the analysis of both static properties and dynamic behaviors of cells/nuclei. While simple approaches such as intensity thresholding or clustering can be used for segmentation of some images, they fail to produce reliable segmentation for biomedical images with often low signal to noise ra-

tio, indistinct object borders, significant topological shape changes, varying object and background intensities. For the segmentation of fluorescently tagged HeLa cell nuclei we used level set-based multi-phase fast graph partitioning active contours (FastGPAC). FastGPAC is our efficient implementation of graph partitioning active contours (GPAC), that reduces the $O(N^4)$ computational complexity and memory requirements of the original GPAC algorithm to $O(N^2)$ computational complexity and constant memory requirement ($O(nL)$) where N^2 is the image size, L is number of histogram bins, and n is the number of phases. Histogram-based region-descriptors (instead of means or variances which may result in poor representation, canceling or blending effects) and flexible distance measure selection provide GPAC and FastGPAC several advantages compared to the widely used Chan & Vese's region-based active contour model [4].

A. GPAC-Graph Partitioning Active Contours

Graph partitioning active contours (GPAC) is introduced in [12] as a new curve evolution framework. This variational framework is based on pairwise similarities or dissimilarities between points. The initial across region cuts cost in [12] is recently reformulated in terms of pairwise dissimilarities within regions in [1]. GPAC can be used within parametric snake-based or implicit level set-based active contour paradigms. Level set-based active contours provide advantages such as eliminating the need to reparameterize the curve and automatic handling of topology changes [11]. In level set-based active contour methods, a curve $\mathcal{C}$ ($\mathcal{C} = \partial r$, boundary of an open set $r \in \Omega$) is represented implicitly via a Lipschitz function $\phi : \Omega \mapsto \mathbb{R}$ by $\mathcal{C} = \{(x, y)|\phi(x, y) = 0\}$. Heaviside function is used as an indicator function for the points inside and outside the curve $\mathcal{C}$. The GPAC energy function is written as:

$$E_{WR} = \iint_{\Omega}\iint_{\Omega} w(p_1,p_2)H(\phi(p_1))H(\phi(p_2))dp_1dp_2 + \iint_{\Omega}\iint_{\Omega} w(p_1,p_2)\Big(1-H(\phi(p_1))\Big)\Big(1-H(\phi(p_2))\Big)dp_1dp_2 \quad (1)$$

where $H(\phi)$ and $1 - H(\phi)$ refer to interior and exterior regions of the curve $\mathcal{C}$ ($R_i(\mathcal{C})$ and $R_o(\mathcal{C})$) and $w(p_1, p_2)$ is a dissimilarity measure between points p_1 and p_2.
Additional geometric properties or constraints can be introduced into curve evolution by multiplying the two integrals in Eq. 1 with weights α and β [1], [12]. For regularization mean curvature flow $\mathcal{K} = \operatorname{div}\frac{\nabla\phi}{|\nabla\phi|}$ [4] is used. Complete curve evolution equation for GPAC then becomes:

$$\frac{\partial\phi(p_2)}{\partial t} = \delta(\phi(p_2))[\lambda_2\beta\iint_{\Omega} w(p_1,p_2)\Big(1-H(\phi(p_1))\Big)dp_1 - \lambda_1\alpha\iint_{\Omega} w(p_1,p_2)H(\phi(p_1))dp_1 + \mu\operatorname{div}(\frac{\nabla\phi(p_2)}{|\nabla\phi(p_2)|})] \quad (2)$$

which is discretized as:

$$\frac{\Delta\phi(p_2)}{\Delta t} = \delta_\epsilon(\phi(p_2))[\lambda_2\beta\sum_{p_1\in R_o(\mathcal{C})} w(p_1,p_2) - \lambda_1\alpha\sum_{p_1\in R_i(\mathcal{C})} w(p_1,p_2) + \mu\mathcal{K})] \quad (3)$$

B. FastGPAC-Fast Graph Partitioning Active Contours

While powerful in terms of region description, heavy computational and memory requirements prevent GPAC's direct application to large images. Some *approximations* of the algorithm have been proposed in [12] and [1] to alleviate this problem by partitioning the input image into regular blocks or into "superpixels" and by calculating the dissimilarities at block or superpixel level respectively.
The bottleneck in the original GPAC implementation, is the calculatation of the 2D inside and outside sums:

$$\sum_{p_o\in R_o(\mathcal{C})} w(p_o,p_2) \text{ and } \sum_{p_i\in R_i(\mathcal{C})} w(p_i,p_2) \quad (4)$$

where dissimilarity of each point p_2 to each inside point p_i and to each outside point p_o are computed and summed over the corresponding regions. For speed up, dissimilarity of every image point to every image point are pre-computed and stored in a $N^2 \times N^2$ lookup table W where N^2 is the image size. But this $O(N^4)$ table quickly becomes impractical for large images (i.e. over a terabyte of memory is required for an 1024×1024 grayscale image).
FastGPAC speeds up the integral/sum computations by using two additional data structures, histograms $\mathbf{h}_i$ and $\mathbf{h}_o$ for $R_i(\mathcal{C})$, $R_o(\mathcal{C})$ interior and exterior regions of the curve $\mathcal{C}$ respectively. When the point to point (dis)similarity measure $w(p_1, p_2)$ does not incorporate spatial distance between points p_1 and p_2, $w(p_1, p_2)$ can be rewritten as:

$$w(p_1,p_2) \equiv D(F(p_1),F(p_2)) \quad (5)$$

where $F(p)$ is a feature extracted from the point $p(x, y)$, and D is a similarity/dissimilarity measure defined on F (i.e. for absolute grayscale intensity difference, $w(p_1, p_2) = |I(p_1) - I(p_2)|$, feature $F(p)$ is grayscale intensity $I(p)$ and the dissimilarity measure D is L_1 metric.)
GPAC Region Sum Theorem: For cases where the (dis)similarity measure $w(p_1, p_2)$ does not incorporate spatial distance between points p_1 and p_2, the 2D sums, $\sum_{p_i\in R_i} w(p_i, p_2)$ and $\sum_{p_o\in R_o} w(p_o, p_2)$, can be reduced to 1D sums independent of the spatial size or shape of the regions $R_i(\mathcal{C})$ and $R_o(\mathcal{C})$:

$$\sum_{p_r\in R_r} w(p_r,p_2) \equiv \sum_{j=0}^{L-1} h_r(j)\times D(F(p_2),j) \quad (6)$$

where $\mathbf{h}_r$ is the histogram of the feature F in the r^{th} region R_r, $D()$ is a (dis)similarity measure, L is number of bins in $\mathbf{h}_r$, and $h_r(j) = \sum_{p_r\in R\wedge F(p_r)=j} 1$ is the j^{th} bin of $\mathbf{h}_r$ corresponding to the number of points $p_r \in R_r$ whose feature $F(p_r) = j$. In the more general case, $D(F(p_2), j)$ is

replaced by $D(F(p_2), C(j))$ where $C(j)$ is a representative value for the histogram bin $h(j)$.
See [2] for proof and detailed complexity analysis.
Using the GPAC region sum theorem, FastGPAC transforms the discretized curve evolution equation of GPAC Eq. 3 into:

$$\frac{\Delta\phi(p_2)}{\Delta t} = \delta_\epsilon(\phi(p_2))\Big[\lambda_2\beta\sum_{j=0}^{L-1}h_o(j)\times D(F(p_2),j) \tag{7}$$
$$-\lambda_1\alpha\sum_{j=0}^{L-1}h_i(j)\times D(F(p_2),j)+\mu\mathcal{K}\Big]$$
$$=\delta_\epsilon(\phi(p_2))\Big[\sum_{j=0}^{L-1}[\lambda_2\beta\ h_o(j)-\lambda_1\alpha\ h_i(j)]\times D(F(p_2),j)+\mu\mathcal{K}\Big]$$

This transformation reduces the original $O(N^4)$ GPAC computational complexity ($O(N^2)$ for N^2 pixels) to $O(LN^2)$ FastGPAC computational complexity($O(L)$ for N^2 pixels))

C. Extension to Multi-Phase

The two phase segmentation scheme described above is appropriate for segmentation of single class objects/appearances from a single class background. Because of the variability in nuclei appearances during the different stages, we use a multi-phase in this case 4-phase segmentation. This not only improves nuclei detection, but also gives a preliminary information on cell cycle phase, that is exploited during cell tracking and lineage construction.
In [1], GPAC is extended to multi-phase in a way similar to Vese and Chan's multi-phase extension [13] of their two-phase level set image segmentation algorithm [4]. In this scheme, 4-phase (2 level set) GPAC energy function is written as:

$$E_{WR} = \iint_\Omega\iint_\Omega w(p_1,p_2)[\chi_1(p_1)\chi_1(p_2)]dp_1dp_2 \tag{8}$$
$$+\iint_\Omega\iint_\Omega w(p_1,p_2)[\chi_2(p_1)\chi_2(p_2)]dp_1dp_2$$
$$+\iint_\Omega\iint_\Omega w(p_1,p_2)[\chi_3(p_1)\chi_3(p_2)]dp_1dp_2$$
$$+\iint_\Omega\iint_\Omega w(p_1,p_2)[\chi_4(p_1)\chi_4(p_2)]dp_1dp_2$$

where the indicator functions χ_{1-4} for the four regions are:

$$\chi_1(p)=H(\phi_1(p))H(\phi_2(p)); \quad \chi_2(p)=H(\phi_1(p))H^c(\phi_2(p))$$
$$\chi_3(p)=H^c(\phi_1(p))H(\phi_2(p)); \quad \chi_4(p)=H^c(\phi_1(p))H^c(\phi_2(p))$$

and $H^c(\phi(p)) \equiv (1-H(\phi(p)))$. Curve evolution for this multiphase energy function is then:

$$\frac{\partial\phi_1(p_2)}{\partial t} = \delta(\phi(p_2))\Big\{H(\phi_2(p_2))\cdot \tag{9}$$
$$\Big[\iint_\Omega w(p_1,p_2)\chi_3(p_1)dp_1-\iint_\Omega w(p_1,p_2)\chi_1(p_1)dp_1\Big]$$
$$+(1-H(\phi_2(p_2)))\cdot$$
$$\Big[\iint_\Omega w(p_1,p_2)\chi_4(p_1)dp_1-\iint_\Omega w(p_1,p_2)\chi_2(p_1)dp_1\Big]\Big\}$$
$$\frac{\partial\phi_2(p_2)}{\partial t} = \delta(\phi(p_2))\Big\{H(\phi_2(p_2))\cdot \tag{10}$$
$$\Big[\iint_\Omega w(p_1,p_2)\chi_2(p_1)dp_1-\iint_\Omega w(p_1,p_2)\chi_1(p_1)dp_1\Big]$$
$$+(1-H(\phi_2(p_2)))\cdot$$
$$\Big[\iint_\Omega w(p_1,p_2)\chi_4(p_1)dp_1-\iint_\Omega w(p_1,p_2)\chi_3(p_1)dp_1\Big]\Big\}$$

Note that the normalization and regularization terms are ignored for simplicity of the notation, otherwise these terms needs to be included like in Eq. 2. As in the 2-phase case, using the GPAC region sum theorem, FastGPAC transforms this curve evolution equation into its more efficient form:

$$\frac{\Delta\phi_1(p_2)}{\Delta t} = \delta_\epsilon(\phi_1(p_2))\Big\{H(\phi_2(p_2))\cdot\sum_{j=0}^{L-1}[h_3(j)-h_1(j)]D(F(p_2),j)$$
$$+(1-H(\phi_2(p_2)))\cdot\sum_{j=0}^{L-1}[h_4(j)-h_2(j)]D(F(p_2),j)\Big\} \tag{11}$$
$$\frac{\Delta\phi_2(p_2)}{\Delta t} = \delta_\epsilon(\phi_2(p_2))\Big\{H(\phi_1(p_2))\cdot\sum_{j=0}^{L-1}[h_2(j)-h_1(j)]D(F(p_2),j)$$
$$+(1-H(\phi_1(p_2)))\cdot\sum_{j=0}^{L-1}[h_4(j)-h_3(j)]D(F(p_2),j)\Big\} \tag{12}$$

where $h_1,..,h_4$ denote the regional histograms corresponding to the regions $\chi_1,..,\chi_4$.

D. Preprocessing, Shape Analysis, Preclassifier

Preprocessing step filters the raw image sequence using mathematical morphology operations. Noise is reduced, nuclei borders are smoothened, and intra-cellular details are reduced using morphological opening and closing by reconstruction operations [14]. Shape analysis and preclassifier module, converts the 4-phase output of the segmentation module, to a 2-phase mask with detached blobs and some preliminary blob class information to be used by tracking module. Simply flattening the 4-phases into 2-phases by merging three foreground phases of the 4-phase mask would not only result in loss of information but also in unwanted nuclei merges which would disrupt the tracking process. The module recolors 4-phase masks using mean phase intensity to ensure consistent labeling (as black-red-green-yellow in order of increasing intensity), since level set phase assignment can change from frame to frame. Once the consistent labeling is obtained, a rule-based system consisting of morphology, topology, and shape operators, convert the 4-phase mask into 2-phase mask, detach the merged blobs, and classify the blobs based on intensity distribution. These classes do

not necessarily correspond to the cell cycle phases, but they nevertheless provide clues to the tracking module about pre-mitosis and post-mitosis cells.

III. Tracking-based Lineage Analysis

Persistent tracking is an important step in long term behavior analysis such as cell cycle analysis and lineage construction. For lineage analysis we use an extended version of our explicit correspondence-based cell tracking algorithm [3], [9]. This enables us to efficiently control each cell association and handle large amounts of displacements. The tracking module consists of two main sub-modules: (1) Correspondence Analysis, and (2) Segment Generation and Lineage Construction.

(1) In *Correspondence Analysis Module* a graph structure called ObjectMatchGraph is formed where connected components/blobs produced by shape analysis and preclassifier module constitute the nodes of the graph. The link of the graphs are established by cell-to-cell temporal correspondence analysis process which consists of four major steps: 1) object to object distance computation; 2) match confidence matrix construction; 3) absolute match pruning; 4) bi-directional relative match pruning [9].

As association strategy a multi-hypothesis approach with delayed decision is used. Rather than picking a single best match, for each node many possible matches are kept and gradually pruned, as more information becomes available. Besides one-to-one object matches, this scheme supports many-to-one, one-to-many, many-to-many, one-to-none, or none-to-one matches that may result from false detections, or false associations, segmentation errors, occlusion, entering, exiting, or dividing cells.

(2) The *Segment Generation and Lineage Construction Module* has three main steps:

(a) *Node Classification:* The cells/objects in each frame (nodes in the ObjectMatchGraph) are classified based on their number of parent and child objects.

(b) *Segment Generation: Trajectory segments* are formed by tracing the nodes of the ObjectMatchGraph. A linked list of inner nodes (one parent-one child), starting with a source (no parent) or split (many children) type node and ending with a merge (many parent) or sink (no child) type node, are identified and organized in a data structure called *SegmentList*.

(c) *Segment Labeling & Lineage Construction:* Extracted trajectory segments are labeled using a method similar to connected component labeling where parents' labels are propagated to their children. In case of multiple parents, if the parents' labels are inconsistent, then the smaller label (older trajectory) is kept and a flag is set indicating the inconsistency.

A final validation and filtering module analyzes trajectory segments using accumulated evidence such as temporal persistence, size, shape etc. and preliminary blob class information produced by Shape Analysis & Preclassifier module.

IV. Experimental Results

Genetically modified human HeLa Kyoto cell lines were generated and validated to stably express the fused protein green fluorescent protein-tagged proliferating cell nuclear antigen (GFP-PCNA). The first step involved creating HeLa Kyoto lines containing a stably integrated Flp-recombination site (FRT). This was followed by site-specific integration of a construct containing the human EF1α promoter to drive expression of the fusion gene, in this case GFP-PCNA, and a blasticidin resistance marker gene used for selection of the transgenic cells flanked by FRT sites.

Live cell analysis was performed by plating the cells on chambered glass coverslips mounted onto the microscope stage. Images were acquired every 15 minutes using a Zeiss LSM 510 Meta laser scanning confocal microscope using the 488 nm laser line of an Argon ion laser at low power. The spatial dimensions of the images were 1024 x 1024 pixels with a pixel size of 0.2 x 0.2 micron. Three image sequences with 174 frames each have been analyzed.

Figure 2 shows sample segmentation results for frames #1,#33,#121 from the 2TS sequence using 4-phase FastGPAC method. When the 4-phase segmentation masks are recolored (according to mean level set phase intensity) as in 3rd row, some observations on the color scheme can be made i.e. just before mitosis nuclei appear as solid red blobs (fluorescent intensity fade), just after mitosis daughter nuclei appear as red blob with green centers. These observations can be used during lineage construction as an additional information besides frame-to-frame cell correspondences. The evolutions of three cells #3,#7,#13, and their segmentation, tracking results are zoomed and shown in Figure 3.

Tracking results for Seq.3TS and Seq.5TS are shown in Figure 4. Nuclei originating from the same cell (through multiple rounds of mitosis) share the same label and color. The segmentation and tracking results of Seq:5TS have been manually validated. Summary of the segmentation and tracking validation statistics is given in Table I. 157 out of 174 frames were segmented successfully. Among the discarded 17 frames 10 were severely out-of-focus frames and 7 were under-segmented frames. The proposed algorithms detected a total of 4111 nuclei images in 157 frames, no nuclei were missed (false negatives in the table are caused by under-segmentation). Fragmentation caused 6 false splits and 5 merges. 21 out of 22 mitosis events were detected successfully.

V. Conclusions

Current chemical biology methods for studying the spatiotemporal correlation between cell cycle and molecular

TABLE I: Summary of segmentation and tracking statistics for Seq.5TS.

Segmentation Stats		Tracking Stats	
Cells Ground Truth	4103	Mitosis Ground Truth	22
Cells Detected	4111	Mitosis Detected	21
False Negative	2	False Merges	5
False Positive	10	False Splits	6
		Identity Switch	0

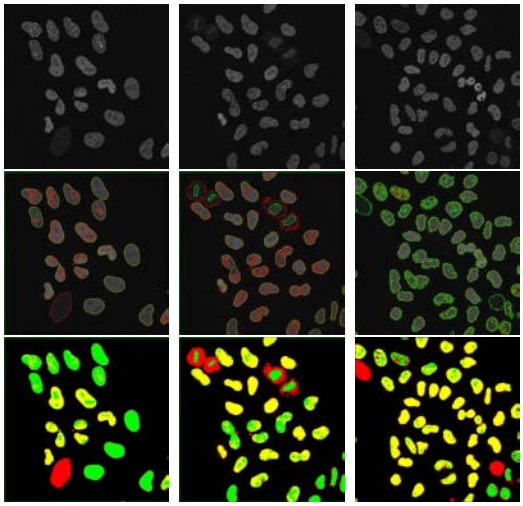

Fig. 2: Sample 4-Phase FastGPAC segmentation results for frames 1,33,121 from the 2TS seq. Top: Original frames; Middle: Level set contours on the preprocessed image; Bottom: Recolored level set masks (black-red-green-yellow in the order of increasing average phase intensity).

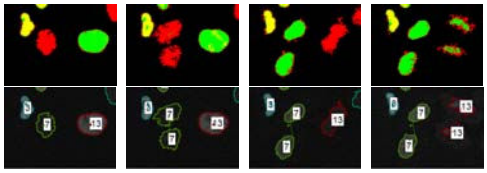

Fig. 3: Sample tracking result showing two mitosis. Left to right frames #3,#5,#11,#13 of Seq.2TS

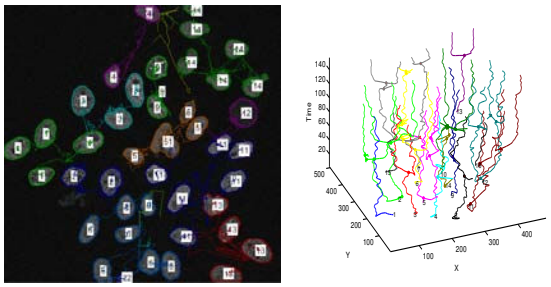

Fig. 4: Tracking results for sequences 3TS (2D view on the last frame) and 5TS (3D view).

structures within the cell nucleus use fluorescence-based imaging of fusion proteins. Often the proteins of interest are involved in basic cellular processes such as DNA synthesis, repair, and replication, which produce temporally varying fluorescence patterns of different sized foci. In the case of GFP-PCNA fusion proteins during the mitosis stage of the cell cycle the cell nuclei virtually disappear. The Poisson imaging noise, lower SNR especially for some phases of the cell cycle, complex non-homogeneous punctuate textural patterns, significant shape changes during cell division and large data volumes required the development of a multi-class region-based segmentation algorithms with topological flexibility. The recently proposed GPAC algorithm solves a graph-based image segmentation problem using an active contour formulation. We extended the multiphase GPAC algorithm for fluorescence-based cell segmentation by incorporating density functions to capture the variability of regions for reliable and accurate segmentation. GPAC has not been previously applied to large biomedical segmentation applications due to extensive memory and computational requirements on the order of a few terabytes for a megabyte-sized fluorescence image. We derive a FastGPAC algorithm that requires constant memory and is highly scalable for high-throughput screening of 2D and 3D time-lapse video microscopy images. Preliminary results indicate that the multiphase implementation is able to segment and accurately track the lineage of fluorescently labeled proliferating cells for more than 32 hours with high precision and recall. Once the cell trajectories are accurately established then the recognition and characterization of specific cell cycle phases can proceed using supervised classification techniques from pattern recognition and machine learning.

REFERENCES

[1] L. Bertelli, B. Sumengen, B. Manjunath, and F. Gibou. A variational framework for multi-region pairwise similarity-based image segmentation. *IEEE Trans. Pattern Anal. Machine Intell.*, 30(8):1400–1414, 2008.

[2] F. Bunyak and K. Palaniappan. Efficient segmentation using feature-based graph partitioning active contours (GPAC). In *Proc. IEEE Int. Conf. Computer Vision*, Kyoto, Japan, Sep. 2009.

[3] F. Bunyak, K. Palaniappan, S. Nath, T.I.Baskin, and G.Dong. Quantitative cell motility for *in vitro* wound healing using level set-based active contour tracking. In *Proc. IEEE Int. Symp. Biomedical Imaging*, pages 1040–1043, Arlington, VA, April 2006.

[4] T. Chan and L. Vese. Active contours without edges. *IEEE Trans. Image Proc.*, 10(2):266–277, Feb. 2001.

[5] X. Chen, X. Zhou, and S. Wong. Automated segmentation, classification, and tracking of cancer cell nuclei in time-lapse microscopy. *IEEE Trans. Biomedical Engineering*, 53(4):762–766, April 2006.

[6] H. Easwaran, H. Leonhardt, and M. Cardoso. Cell cycle markers for live cell analyses. *Cell Cycle*, 4(3):453–455, Mar 2005.

[7] I. Ersoy, F. Bunyak, K. Palaniappan, M. Sun, and G. Forgacs. Cell spreading analysis with directed edge profile-guided level set active contours. *Lecture Notes in Computer Science (MICCAI)*, 5241:376–383, 2008.

[8] K. Li, E. D. Miller, M. Chen, T. Kanade, L. E. Weiss, and P. G. Campbell. Cell population tracking and lineage construction with spatiotemporal context. *Medical Image Analysis*, 12(5):546–566, October 2008.

[9] S. Nath, F. Bunyak, and K. Palaniappan. Robust tracking of migrating cells using four-color level set segmentation. *Lecture Notes in Computer Science (ACIVS)*, 4179:920–932, Sep. 2006.

[10] D. Padfield, J. Rittscher, N. Thomas, and B. Roysam. Spatio-temporal cell cycle phase analysis using level sets and fast marching methods. *Medical Image Analysis*, 13:143–155, Feb. 2009.

[11] J. Sethian. *Level Set Methods and Fast Marching Methods: Evolving Interfaces in Computational Geometry, Fluid Mechanics, Computer Vision, and Materials Science*. Cambridge University Press, 1999.

[12] B. Sumengen and B. S. Manjunath. Graph partitioning active contours (GPAC) for image segmentation. *IEEE Trans. Pattern Anal. Machine Intell.*, 28(4):509–521, Apr 2006.

[13] L. Vese and T. Chan. A multiphase level set framework for image segmentation using the Mumford and Shah model. *Int. J. Computer Vision*, 50(3):271–293, 2002.

[14] L. Vincent. Morphological grayscale reconstruction in image analysis:applications and efficient algorithms. *IEEE Trans. Image Process.*, 2:176–201, Apr. 1993.

[15] M. Wang, X. Zhou, F. Li, J. Huckins, R. King, and S. Wong. Novel cell segmentation and online svm for cell cycle phase identification in automated microscopy. *Bioinformatics*, 24(1):94–101, Jan. 2008.